Rheinische Friedrich-Wilhelms-Universität Bonn

Advanced Laboratory Course

Performed on: April 4th - 5th, 2022

Submitted on: May 3, 2022

A249: Laser Gyroscope

Authors
Paarth Thakkar
Keito Watanabe

Tutor(s)
Thorsten Groh
Marc Vöhringer

Abstract

Contents

1 Introduction **2**

2 Theory **3**

2.1 Gyroscopes . . . 3

2.1.1 The Sagnac Effect . . . 3

2.1.2 Ring Laser Gyroscopes . . . 4

2.2 Optical Cavities . . . 5

2.2.1 Finesse . . . 5

2.2.2 Lock-In Effect . . . 5

2.3 Allan Deviation . . . 5

3 Pre-Lab Exercises **6**

4 Set-up and Procedure **7**

5 Results and Discussion **8**

6 Conclusion and Outlook **9**

7 Acknowledgements **10**

8 Appendix **11**

Chapter 1

Introduction

Chapter 2

Theory

2.1 Gyroscopes

2.1.1 The Sagnac Effect

The Sagnac effect tells us that whilst the motion between two inertial frames cannot be distinguished, two rotating frames can be distinguished, allowing one to directly measure the rotation rate of an inertial system [1]. This effect was first observed by George Sagnac in 1913, whom believed that this experiment was a proof that aether exists in an inertial frame [2]. This, however, was disproven by Max von Laue in 1911 where he showed that the Sagnac effect was compatible with special relativity [3]. However, the interpretation of the Sagnac effect due to the general theory of relativity is still investigated today, even though it is already well-known in literature [4]. In our analysis, we utilize the Sagnac effect on a gyroscope to measure the rotation rate of the Earth.

To observe the Sagnac effect, we consider an interferometer setup with light propagating with wavelength λ enclosing an area $\vec{A}$ with perimeter P. Placing such a setup onto a rotating platform with frequency $\vec{\Omega}$, we observe that the optical path that each light travels changes. For example, if the table rotates counter-clockwise, then the path of the co-rotating light increases, while that of the other light decreases (see Fig. 2.1.1). The Sagnac effect then tells us the resulting phase shift between the two lights:

$$\delta\phi = \frac{8\pi \vec{A} \cdot \vec{\Omega}}{c\lambda} \propto \vec{A} \cdot \vec{\Omega} \tag{2.1.1}$$

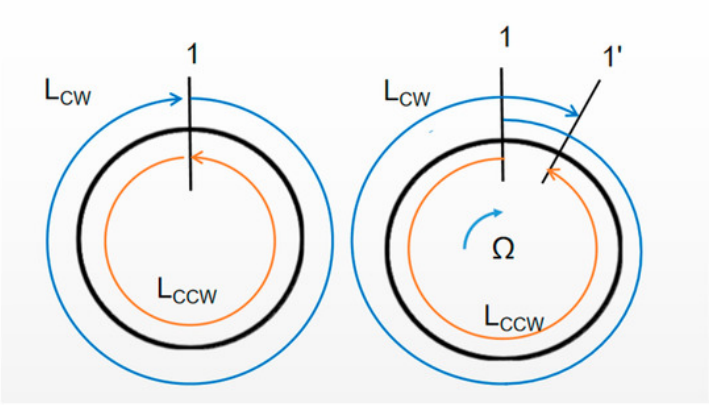

Figure 2.1.1: The Sagnac effect. *Left*: Setup without rotation. The beam moving clockwise (blue) and counter-clockwise (orange) have the same optical path length. *Right*: Setup with a clockwise rotation Ω. The path length of the clockwise beam is larger than that of the counter-clockwise beam [5].

A more detailed derivation using the relativistic law of velocity addition can be found in Ref. [4].

2.1.2 Ring Laser Gyroscopes

Active Ring Laser Gyroscopes

In order to incorporate the Sagnac effect within our experiment, we utilize ring laser gyroscopes. A laser is placed within an enclosed cavity, and emits two counter-propagating beams. Such beams reflect off mirrors and interfere at the end of their propagation. When rotating the platform in which such setup is placed, different interference patterns can be observed, and transforms the ring cavity system into a cavity resonator. The corresponding beat frequency $\delta\nu$ observed is then the Sagnac frequency, which is given as such:

$$\delta\nu = \frac{4\vec{A}\cdot\vec{\Omega}}{P\lambda} \tag{2.1.2}$$

In our experiment, we only consider square ring cavities so that $A = L^2$ and $P = 4L$, where L is the path length of each arm. As such, we can simplify Eq. 2.1.2 as such:

$$\delta\nu = \frac{L\Omega}{\lambda} = n\Omega \tag{2.1.3}$$

where $n = L/\lambda$ is the number of nodes of the light field in each arm. Thus the Sagnac frequency is proportional to the rotation rate of the inertial system [1].

Passive Ring Laser Gyroscopes

In contrast to the active ring laser gyroscope, in which the laser is contained within the ring cavity, the passive ring laser gyroscope places the laser source outside of the cavity system. In this system, the external laser is locked to the counter-propagating modes of the resonator. By placing the laser outside of the resonator, we can reduce the systematic effects due to the lasing medium and the lock-in effect (see Sec. 2.2.2), and also increase the available light power for the beam. This method, however, also introduces an added complexity of laser locking [1]. See Fig. 2.1.2 for a comparison between the two systems. In our experiment, we use the passive ring laser gyroscope and thus laser locking becomes an importance in our measurements.

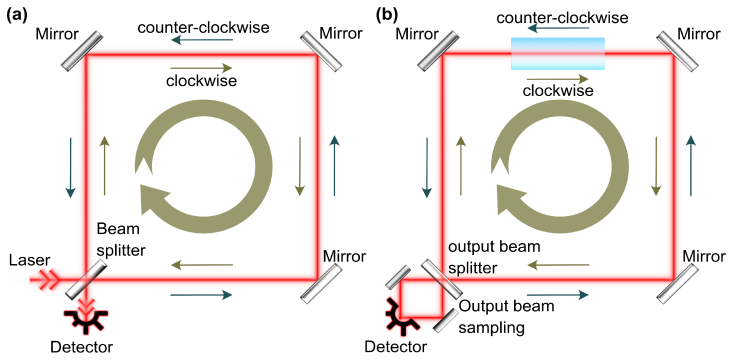

Figure 2.1.2: A *Left*: passive and *Right*: active ring laser gyroscope system [6].

Gyroscope Sensitivity

The sensitivity of the ring laser gyroscope depends on a variety of factors, namely the wavelength λ, arm length L, finesse F of the resonator (see Sec. 2.2.1), and the shot-noise limited detection given by the number of photons $N = P_{\text{opt}}/h\nu = P_{\text{opt}}\lambda/hc$ detected per unit time. P_{opt} represents the optical power given to the laser. Combining all such factors, we obtain the sensitivity of the ring laser gyroscope for an integration time τ as such:

$$\delta\Omega = \frac{1}{4}\frac{c}{L^2F}\sqrt{\frac{ch\lambda}{P_{\text{opt}}}}\frac{1}{\tau} \tag{2.1.4}$$

This gyroscope sensitivity can be directly compared with the Allan deviation σ_{ad} that determines the instability of a measurement for some averaged integration time τ (see Sec. 2.3). The best gyroscope sensitivity observed was from the G-ring at the German Fundamentalstation Wettzell with a sensitivity of around 12 prad / s / $\sqrt{\text{Hz}}$ [1].

2.2 Optical Cavities

2.2.1 Finesse

2.2.2 Lock-In Effect

2.3 Allan Deviation

Chapter 3

Pre-Lab Exercises

Before conducting the experiment, we were required to determine the rotation rate of the Earth using our phone. Our phones contain a microelectromechanical system (MEMS), which is a portable and inexpensive inertial sensor that track the motion of the phone. Using the application `phyphox` constructed by RWTH Aachen University, we evaluated the capabilities of the MEMS gyroscope within the iPhone 13.

Chapter 4

Set-up and Procedure

Chapter 5

Results and Discussion

Chapter 6

Conclusion and Outlook

Chapter 7

Acknowledgements

Chapter 8

Appendix